Using the spleen for time-delay correction of the input function in measuring hepatic blood flow with oxygen-15 water by dynamic PET

Hiroki Taniguchi, Akihiro Yamaguchi, Satoshi Kunishima,
Toshimori Koh, Mamoru Masuyama, Hiroshi Koyama,
Atsushi Oguro and Hisakazu Yamagishi

First Department of Surgery, Kyoto Prefectural University of Medicine

By the spleen, we calculated a time-delay correction of the input function for quantitation of hepatic blood flow with oxygen-15 water and dynamic positron emission tomography. The time delay (Δt) between the sample site and the spleen was calculated based on nonlinear multiple regression analysis when splenic blood flow was determined. Then hepatic blood flow was quantified by a method using the input function and incorporating Δt, which was assumed to be equal to the time delay between the sample site and the liver. Then hepatic arterial and portal blood flows were estimated separately as well as the delay time for passage within the organs of the portal circulation. The mean coefficient of variation and the mean sum of squares of errors decreased to about 70% when total hepatic blood flow was calculated from the results for regions of interest in three slices of the same liver segment. We concluded that using the spleen for time-delay correction of the input function for measuring hepatic blood flow by this method gave satisfactory results.

Key words: regional hepatic blood flow, oxygen-15 water, positron emission tomography, spleen

INTRODUCTION

IN MEASURING cerebral blood flow by means of a [^{15}O]-H$_2$O bolus injection dynamic positron emission tomographic (PET) study, a time-delay correction is calculated between the brain and the arterial sampling site, usually the radial or brachial artery. Several methods have been described for accomplishing this correction,[1–3] but these methods cannot be extrapolated to simultaneous quantitation of the hepatic arterial and portal blood flow, and the complexities of the liver's dual blood supply require appropriate correction. We previously have described several evolving models for quantitation of hepatic blood flow by means of [^{15}O]-H$_2$O dynamic

PET.[4,5] We also have measured splenic blood flow, because the spleen is included in images obtained during hepatic PET studies.[6,7] In the present study, we performed time-delay correction of the input function by using the spleen to assess hepatic blood flow with [^{15}O]-H$_2$O-bolus-injection dynamic PET.

THEORY, MATERIALS AND METHODS

Theory

We based this study on our previous models. The original simple model may be expressed in the following three equations.[4] When organs draining into the portal vein are considered to be one organ (the "portal organ"), the rate of change of the tracer in the portal organ and the liver can be expressed as Equations 1 and 2 respectively. The sum of arterial blood flow and portal blood flow represents total hepatic blood flow (Eq. 3):

$$\frac{dCp(t)}{dt} = fp \times Ca(t) - fp \times \frac{Cp(t)}{Kp} \qquad \text{Eq. 1}$$

$$\frac{dCh(t)}{dt} = fa \times Ca(t) + fp \times \frac{Cp(t)}{Kp} - fh \times \frac{Ch(t)}{Kh} \quad \text{Eq. 2}$$

$$fh = fa + fp \quad \text{Eq. 3}$$

In these equations, fa and fp (mL/sec/g) represent hepatic arterial blood flow and portal venous blood flow, respectively. $Ca(t)$, $Cp(t)$ and $Ch(t)$ (counts/sec/mL) are the tracer concentrations in the arterial blood, the portal organ, and the liver, respectively. Kh and Kp are the tracer's blood equilibrium partition coefficients for the liver and portal organ, respectively.

In a subsequent modification the model included a coefficient for portosystemic shunting, as well as a coefficient for circulation time within the portal organ.[5] The tracer concentration in the liver was also separated into arterial and portal components. The dynamics of the tracer could be explained in terms of the following four equations. Equation 1 is unchanged from the simple model. When radioactivity in the liver is separated into flow from the hepatic artery and flow from the portal vein, with $Cha(t)$ representing the former and $Chp(t)$ the latter, Equation 2 can be subdivided into the following two Equations, 4 and 5. Equation 5 then includes coefficients for portosystemic shunting and circulation time within the portal organ.

$$\frac{dCp(t)}{dt} = fp \times Ca(t) - fp \times \frac{Cp(t)}{Kp} \quad \text{Eq. 1}$$

$$\frac{dCha(t)}{dt} = fa \times Ca(t) - fa \times \frac{Cha(t)}{Kha} \quad \text{Eq. 4}$$

$$\frac{dChp(t)}{dt} = E \times fp \times \frac{Cp(t+\tau)}{Kp} - E \times fp \times \frac{Chp(t)}{Khp} \quad \text{Eq. 5}$$

$$Ch(t) = Cha(t) + Chp(t), fh = fa + E \times fp \quad \text{Eq. 6}$$

In these equations, fa and $E \cdot fp$ (mL/sec/g) represent tracer flows into the liver by way of the hepatic artery and from the portal circulation (portal organ), respectively. $Ca(t)$, $Cp(t)$, and $Ch(t)$ (counts/sec/mL) are the tracer concentrations in the arterial blood, the portal organ, and the liver, respectively. $Cha(t)$, and $Chp(t)$ (counts/sec/ mL) represent the radioactivities in the liver contributed by flow from the hepatic artery and flow from the portal vein, respectively. Kha, Khp, and Kp are organ-blood partition coefficients for water in the arterial component of the liver, the portal component of the liver, and the portal organ, respectively. E is the actual ratio of tracer flowing into the liver (1 minus E is therefore a shunting rate), and τ (sec) is the time delay between the detection of tracer radioactivity in the portal organ and its detection in the liver.

For correction of the time delay between the liver and the blood sampling site in the present, further modified model (Fig. 1), we used the spleen. The method for measuring blood flow in the spleen was based on our previously reported study.[6]
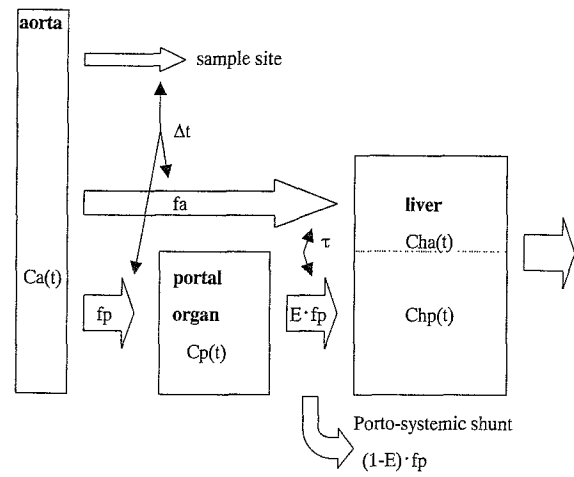
Fig. 1 Scheme for the current model. The terms fa and fp (mL/ sec/g) represent tracer flows into the liver by way of the hepatic artery and from the portal organ, respectively. $Ca(t)$, $Cp(t)$, and $Ch(t)$ (counts/sec/mL) are the tracer concentrations in the arterial blood, the portal organ, and the liver, respectively. $Cha(t)$ and $Chp(t)$ (counts/sec/mL) represent components of radioactivities in the liver, as flow from the hepatic artery and flow from the portal vein, respectively. E is the actual ratio of tracer that flows into the liver, 1 minus E being a shunting rate. The term τ (sec) is the time delay between detection of radioactivity of a radiotracer in the portal organ and in the liver, and Δt is a time delay between the detection of tracer radioactivity in the liver and that at the arterial sampling site, a newly introduced coefficient.

$$\frac{dCs(t)}{dt} = fs \cdot Ca(t) - fs \cdot \frac{Cs(t)}{Ks} \quad \text{Eq. 7}$$

In this equation, fs (mL/sec/g) represents splenic blood flow, and Ks is the spleen-blood equilibrium partition coefficient for the tracer. $Ca(t)$ and $Cs(t)$ (counts/sec/mL) are the tracer concentrations in the arterial blood and the spleen, respectively. When a new coefficient [Δt (sec)] for the time delay between the spleen and sample site is introduced in Equation 7, the expression becomes

$$Cs(t) = fs \cdot \int_0^t Ca(t - \Delta t) \cdot e^{-\frac{fs}{Ks} \cdot (t-x)} dx \quad \text{Eq. 8}$$

As the input function, the following two equations were applied when the splenic blood flow was estimated:

$$Ca(t) = a_1 \cdot e^{b_1 t} - a_2 \cdot e^{b_2 t} \quad [0 \le t \le t_{max}]$$
$$Ca(t) = c_1 \cdot e^{-d_1 t} - c_2 \cdot e^{-d_2 t} \quad [t_{max} \le t] \quad \text{Eq. 9}$$

where t_{max} is the time when the radioactivity concentration in the blood sample is maximum. The terms Δt, fs, and Ks were calculated by using the radioactivity concentration in the arterial blood sample and the time-activity curve for the spleen in Equation 8 and Equation 9 by the simplex method, a nonlinear least-squares method.

Because the spleen usually is included in the imaging field for hepatic PET, the assumption that Δt is nearly equal to the time delay between the liver and the blood sampling site permits substitution of the following Equa-

First step

Second step
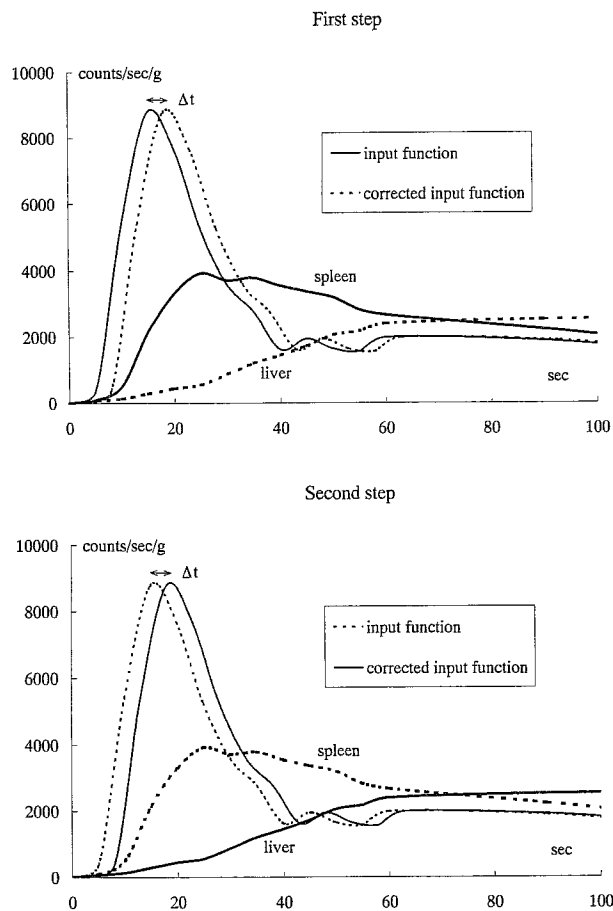
Fig. 2 Method of time-delay correction. Initially, the time delay (Δt) between the sample site and the spleen was calculated using nonlinear multiple regression analysis when the splenic blood flow was quantified. Subsequently, the hepatic blood flow was calculated using the new input function that incorporated Δt.

tions for the hepatic input function:

$$Ca(t) = a_1 \cdot e^{b_1(t-\Delta t)} - a_2 \cdot e^{b_2(t-\Delta t)} \quad [0 \leq t \leq t_{max}]$$
$$Ca(t) = c_1 \cdot e^{-d_1(t-\Delta t)} - c_2 \cdot e^{-d_2(t-\Delta t)} \quad [t_{max} \leq t] \quad \text{Eq. 10}$$

We therefore arrived at Δt by first calculating the splenic blood flow, and we quantified the hepatic blood flow by using the input functions and value for Δt (Fig. 2).

PATIENTS AND METHODS

In 88 patients (48 men and 40 women), regional hepatic blood flow was measured simultaneously in all four liver segments (lateral, medial, anterior, and posterior) by using PET, after informed consent was obtained. The patients ranged in age from 29 to 79 years with a mean age of 57.9 years. All the patients had normal liver function; their liver biopsy specimens or resected liver being diagnosed histologically as normal.

Serial measurements were performed in fasted patients in the supine position in a whole-body PET scanner
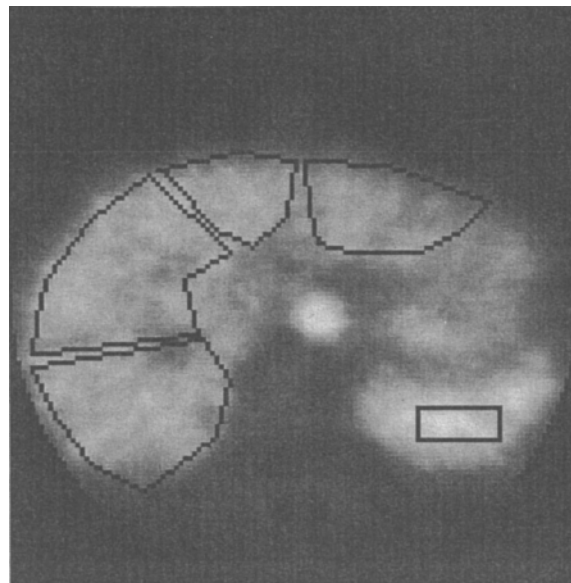
Fig. 3 Regions of interest for the liver segments and the spleen.
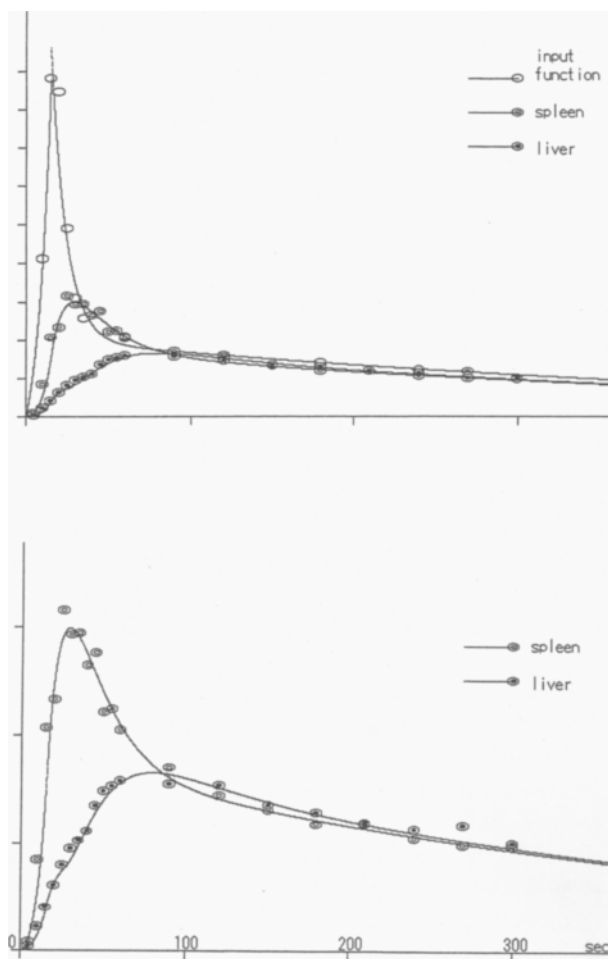
Fig. 4 Actual data from a typical case (top), with y-axis expansion for the spleen and liver at the bottom. The time-activity curve of the liver shows an inflection point within 60 min after injection of [^{15}O]-H$_2$O.

Table 1 Results of the spleen

	Mean	Coefficient of variation
Splenic blood flow (mL/100 g/min)		
without time delay correction	144.8 (127.1–162.6)	17.9 (14.6–21.1)
with time delay correction	133.3 (120.0–146.8)	17.2 (14.0–20.3)
Spleen-blood partition coefficient for water		
without time delay correction	0.710 (0.683–0.736)	11.2 (8.8–13.7)
with time delay correction	0.724 (0.700–0.748)	11.5 (8.7–14.3)
Time delay between the spleen and arterial sample site (sec)		
with time delay correction	2.38 (1.90–2.86)	29.6 (13.1–46.1)

Number in parentheses indicates levels below the 5th and the above 95th percentile.

Table 2 Results of hepatic blood flow obtained using each model

	Lateral segment	Medial segment	Anterior segment	Posterior segment
Arterial hepatic blood flow (mL/100 g/min)				
Simple model	43.6 (40.2–47.0)	38.8 (35.7–41.8)	35.3 (33.0–38.0)	37.0 (34.8–39.2)
Modified model	54.9 (50.4–59.4)	47.1 (43.0–51.3)	40.2 (37.4–42.9)	42.7 (39.6–45.8)
New model	47.0 (43.8–50.3)	39.8 (36.7–42.9)	34.9 (32.8–37.1)	36.7 (34.4–39.0)
Portal hepatic blood flow (mL/100 g/min)				
Simple model	20.7 (17.9–23.4)	32.4 (27.4–37.5)	35.7 (31.2–40.2)	28.6 (24.5–32.6)
Modified model	88.6 (77.2–100.1)	100.2 (89.1–111.3)	95.8 (85.5–106.3)	88.9 (80.1–97.6)
New model	82.3 (73.8–90.8)	86.8 (79.3–94.2)	91.3 (84.4–98.1)	84.0 (77.2–90.8)
Total hepatic blood flow (mL/100 g/min)				
Simple model	64.2 (68.7–59.8)	71.2 (65.7–76.6)	71.2 (67.1–75.4)	65.6 (61.9–69.2)
Modified model	142.3 (129.8–154.8)	145.8 (134.2–157.4)	134.5 (123.6–145.4)	129.5 (120.5–138.6)
New model	129.3 (119.8–138.9)	126.6 (118.3–134.9)	126.2 (118.9–133.4)	120.8 (113.6–127.9)

Mean (levels below the 5th and above the 95th percentile)

(HEADTOME III SET-120W, Shimadzu, Kyoto, Japan). Performance characteristics of the PET system in this study were set to obtain an image resolution of 8.2 mm in full width at half-maximum (FWHM) and a slice thickness of 11 mm (direct) and 13 mm (cross-plane) FWHM. The matrix size of the image was 128 × 128 with a 2-mm pixel size. The slice interval of the planes was 15 mm.

After an intravenous bolus injection of 20 mCi (370 MBq) of the radioisotope [^{15}O]-H$_2$O produced in a medical cyclotron (BC-1710, Japan Steel Works, Muroran, Japan), 12 PET measurements were acquired at serial 5-sec intervals for 1 min, and another 8 measurements were obtained every 30 seconds for the next 4 min. Emission data for three slices at each 1.5-cm thickness were collected simultaneously. The physical decay of ^{15}O was corrected every 2.5 sec. Regions of interest (ROIs) were defined to correspond to the liver segments and the spleen in the PET images (Fig. 3) with reference to computed tomographic images at corresponding levels. In the current study, the specific gravity of the liver and spleen was assumed to be 1.

Blood samples were taken from the left brachial artery at 10, 15, 20, 25, 30, 35, 60, 120, 180, and 240 sec after the beginning of the emission scan, to yield a total of 10 samples in a 4-min period. Radioactivity counts in the blood samples were measured immediately in a precalibrated well counter (MINAXI-γ, Packard Japan;

Tokyo).

Results for the three models were compared by coefficient of variation, which was calculated using the standard deviation and the mean hepatic blood flow of three ROIs set for three serial slices in the same liver segment [coefficient of variation (CV) = 100 × standard deviation/mean], and from the sum of the squares of the errors (SSE) of each result. Hepatic blood flow was assumed to be uniform within the same liver segment. The previously reported result obtained with the simple model[4] was derived from fa, fp, Kp, and Kh with the solution (Eq. 11) of Equations 1, 2, and 3 and the simplex method.

$$Ch(t) = fa \cdot \int_0^t Ca(x) \cdot e^{-\frac{fh}{kh} \cdot (t-x)} dx$$
$$+ \frac{fp \cdot fp}{Kp} \cdot \int_0^t \left\{ \int_0^x Ca(y) \cdot e^{-\frac{fp}{Kp} \cdot (x-y)} dy \right\} \cdot e^{-\frac{fh}{Kh} \cdot (t-x)} dx$$

Eq. 11

The result with the modified model in a previous report[5] was obtained by deriving fa and Kha by the simplex method and with the solution (Eq. 12) of Equations 1, 4, 5, and 6 during the arterial phase (from the beginning of scanning to the maximum point of the time-activity curve of the spleen), and determining fp, Kp, Khp, and E from the beginning of scanning to the time when scanning was complete by using the data already determined (fa and Kha).

Table 3 Results of CVs and SSEs obtained using each model

	Coefficient of variation		Sum of the squares of errors	
	Mean	5–95%	Mean	5–95%
Arterial hepatic blood flow				
Simple model	12.6	11.0–14.3		
Modified model	12.8	11.3–14.4		
New model	13.6	12.4–14.8		
Portal hepatic blood flow				
Simple model	36.3	31.8–40.7		
Modified model	37.8	33.0–42.6		
New model	22.0	19.6–24.4		
Total hepatic blood flow				
Simple model	15.8	14.1–17.5	422958	380337–465579
Modified model	22.6	19.8–25.3	312654	267049–358259
New model	14.2	12.7–15.8	220728	197912–243544

Coefficient of variation = (100 × standard deviation/mean) of results from three slices in the same liver segment
5–95%: levels below the 5th and above the 95th percentile

$$Ch(t) = fa \cdot \int_0^t Ca(x) \cdot e^{-\frac{fa}{Kha} \cdot (t-x)} dx$$

$$+ \frac{E \cdot fp \cdot fp}{Kp} \cdot \int_0^t \left\{ \int_0^{x+\tau} Ca(y) \cdot e^{-\frac{fp}{Kp} \cdot (x+\tau-y)} dy \right\} \cdot e^{-\frac{E \cdot fp}{Khp} \cdot (t-x)} dx$$

Eq. 12

In these two methods, values were approximated by the simplex method with Equation 9 as the input function. In the new method, the splenic blood flow and Δt were calculated with these input functions (Eq. 9) by the simplex method. Then, with the new input functions including Δt (Eq. 10), hepatic blood flow was calculated in the same manner as in the modified method; specifically fa and Kha were calculated by the simplex method from the beginning of scanning to the time of maximal activity in the spleen. Finally, fp, Kp, Khp, and E were calculated by the simplex method from the beginning of scanning to the time of its completion by using the data already determined. The time delay correction for hepatic blood flow was therefore performed by using the splenic result, which is available on the same slice as the liver data.

Data processing was performed by means of a specially developed software program on a personal computer (PC-LW2634A, NEC, Tokyo, Japan). Statistical evaluation was performed with Microsoft Excel 97 (Japan Microsoft, Tokyo).

RESULTS

Splenic blood flow was calculated in 180 ROIs (Table 1). The mean time delay between the spleen and arterial sample site was 2.38 sec. The hepatic blood flow was calculated in 588 ROIs. The actual data from a typical case are shown in Figure 4, and the results of hepatic blood flow based on each of the three models are shown in Table 2. Arterial hepatic blood flow values based on the current model were similar to those obtained with the simple model, but smaller than those obtained with the modified model. Portal hepatic blood flow values obtained with the current model were larger than those obtained with the simple model but smaller than those obtained with the modified model. CVs and SSEs are shown in Table 3. CVs of arterial blood flow based on each model were similar, but the CV for total blood flow based on the current model was smaller than that given with the others because the CV of the portal hepatic blood flow was the smallest among the models. A one-way analysis of variance (ANOVA) demonstrated a significant difference between the three models in SSEs (d.f. = 1763, p < 0.00001). In addition, significant differences were evident between models in the SSE. A p value less than 0.00001 was observed between the result obtained using the modified model and that yielded by the current model by means of a nonparametric Wilcoxon test.

DISCUSSION

The time required for a tracer to circulate from the injection site to the liver will differ according to the time required to reach an arterial sampling site. If the difference is large, the estimated value of the hepatic blood flow will deviate widely from the true value. In our previous models for quantitation of hepatic blood flow, we had ignored this time delay because of the already complicated model needed to reflect the dual blood supply of the liver. Although a time-delay correction is used regularly when cerebral blood flow is measured by PET, we felt that adding a new parameter for time delay to our model that was based on nonlinear multiple regression analysis as used for the brain would result in a larger error.

Since the spleen usually is included in the imaging field when we quantify hepatic blood flow, we studied the possibility of using the spleen to determine the time-delay correction. Accordingly, the mean time delay between the

spleen and arterial sample site was 2.38 sec, the splenic blood flow decreased slightly and the spleen-blood partition coefficient for water increased slightly. These results for splenic blood flow are in agreement with some previous reports.[8-10]

Our new model assumed that the time delays for the liver and spleen were almost the same. First, we attempted to calculate the time delay for the spleen in the same manner as for the brain,[1,11] by nonlinear multiple regression analysis. Then the hepatic blood flow was calculated by using the time delay for the liver added to the input function (Fig. 2). The hepatic blood flow changed equally with the splenic blood flow. The results for the liver were also in agreement with some reported values.[12,13] After introduction of splenic time delay into the hepatic time delay correction, we obtained smaller CVs and SSEs without using additional parameters.

With the time-delay correction, the mean CV of the arterial blood flow was not different from that observed before the correction, but the CV of the portal blood flow was significantly lower when this correction was used. In particular, because the velocity of portal blood flow was low, the time delay more profoundly influenced the measurement results. We believe that this rationale explains why the CV of the portal blood flow based on the current model was smaller than that with earlier models. Furthermore, the decrease in the CV of portal blood flow decreased the CV of total blood flow.

Measuring hepatic arterial and portal blood flow separately is extremely difficult. Ziegler and colleagues[14] have proposed a model that is physiologic for use in measuring hepatic blood flow with [15O]-H2O by PET, but errors in the PET scanning protocol and in data accumulation limited the applicability of that study. A typical time-activity curve of the spleen and the liver (Fig. 4) shows an inflection point where time-activity in the spleen is maximum, thought to represent the first point when the radioactive water reaches the liver in the portal blood flow from the spleen. This point usually is detected within 60 sec after isotope injection. Accordingly, PET should be performed frequently in the first 60 min to detect this inflection point; otherwise separate measurement of arterial and portal blood flow cannot be performed. Moreover, the spleen provides a means of calculating the time-delay correction.

In the past, the kidney was used when hepatic blood flow was measured with radioactive colloid,[15] because colloids can pass through the kidneys but are trapped in the spleen. The current study demonstrates that the spleen is useful for calculation of the time-delay correction. Because in almost all cases the inflection point of the time-activity curve of the liver corresponds exactly to the peak of the time-activity curve of the spleen, we believe that our assumption is correct and that any distortion is minimum. A number of improvements have been made in our method since the first model, and we believe that the time-delay

correction was made successfully, but the assumption considering the various portal organs as a single one still is required, and this point needs further consideration.

REFERENCES

1. Iida H, Higano S, Tomura N, Shishido F, Kanno I, Miura S, et al. Evaluation of regional differences of tracer appearance time in cerebral tissues using [15O] water and dynamic positron emission tomography. *J Cereb Blood Flow Metab* 8: 285–288, 1988.
2. Meyer E. Simultaneous correction for tracer arrival delay and dispersion in CBF measurements by the H2 15O autoradiographic method and dynamic PET. *J Nucl Med* 30: 1069–1078, 1989.
3. van den Hoff J, Burchert W, Müller-Schauenburg W, Meyer GJ, Hundeshagen H. Accurate local blood flow measurements with dynamic PET: Fast determination of input function delay and dispersion by multilinear minimization. *J Nucl Med* 34: 1770–1777, 1993.
4. Taniguchi H, Oguro A, Takeuchi K, Miyata K, Takahashi T, Inaba T, et al. Difference in regional hepatic blood flow in liver segments—Non-invasive measurement of regional hepatic arterial and portal blood flow in human by positron emission tomography with H2 15O —. *Ann Nucl Med* 7: 141–145, 1993.
5. Taniguchi H, Oguro A, Koyama H, Masuyama M, Takahashi T. Analysis of models for quantification of arterial and portal blood flows in the human liver using positron emission tomography. *J Comput Assist Tomogr* 20: 135–144, 1996.
6. Taniguchi H, Oguro A, Koyama H, Miyata K, Takeuchi K, Takahashi T. Determination of spleen-blood partition coefficient for water with oxygen-15-water and oxygen-15-carbon dioxide dynamic PET steady state method. *J Nucl Med* 36: 599–602, 1995.
7. Taniguchi H, Koyama H, Masuyama M, Takada A, Mugitani T, Tanaha H, et al. Angiotensin II-induced hypertension chemotherapy: Evaluation of hepatic blood flow with 15-Oxygen PET. *J Nucl Med* 37: 1522–1523, 1996.
8. Huchzermeyer H, Schmitz-Feuerhake I, Reblin T. Determination of splenic blood flow by inhalation of radioactive rare gases. *Eur J Clin Invest* 7: 345–349, 1977.
9. Peters AM, Klonizakis I, Lavender JP, Lewis SM. Use of 111Indium-labelled platelets to measure spleen function. *Br J Haematology* 46: 587–593, 1980.
10. Manoharan A, Gill RW, Griffiths KA. Splenic blood flow measurements by Doppler ultrasound. *Cardiovascular Res* 21: 779–782, 1987.
11. Iida H, Kanno I, Miura S, Murakami M, Takahashi K, Uemura K. Error analysis of a quantitative cerebral blood flow measurement using H2 15O autoradiography and positron emission tomography, with respect to dispersion of input function. *J Cereb Blood Flow Metab* 6: 536–545, 1986.
12. Yasuhara Y, Miyauchi S, Hamamoto K. A measurement of regional portal blood flow with Xe-133 and balloon catheter in man. *Eur J Nucl Med* 15: 245–250, 1989.
13. Shiomi S, Kuroki T, Ueda N, et al. Measurement of hepatic blood flow by use of perirectal portal scintigraphy with 133Xe. *Nucl Med Commun* 12: 235–242, 1991.

14. Ziegler SI, Haberkorn U, Byrne H, Tong C, Kaja S, Richolt JA, et al. Measurement of liver blood flow using oxygen-15 labeled water and dynamic positron emission tomography: limitations of model description. *Eur J Nucl Med* 23: 169–177, 1996.

15. Fleming JS, Ackery DM, Walmsley BH, Karran SJ. Scintigraphic estimation of arterial and portal blood supplies to the liver. *J Nucl Med* 24: 1108–1113, 1983.